Journal of the Korean Society of Marine Environment & Safety
Research Paper
Vol. 29, No. 6, pp. 672-680, October 31, 2023, ISSN 1229-3431(Print) / ISSN 2287-3341(Online) https://doi.org/10.7837/kosomes.2023.29.6.672

Study of Small Craft Resistance under Different Loading Conditions using Model Test and Numerical Simulations

Jun-Taek, Lim* · Michael** · Nam-Kyun, Im*** · Kwang-Cheol, Seo****†

*, ** Graduate School of Mokpo National Maritime University, Mokpo 58628, Korea
*** Professor, Department of Navigation Science, Mokpo National Maritime University, Mokpo 58628, Korea
**** Professor, Department of Naval Architecture & Ocean Engineering, Mokpo National Maritime University, Mokpo 58628, Korea

모형시험과 수치해석을 이용한 하중조건 변화에 따른 소형선박의 저항성능 변화에 관한 연구

임준택* · 마이클** · 임남균*** · 서광철****†

*, ** 목포해양대학교 대학원, *** 목포해양대학교 항해학부 교수, **** 목포해양대학교 조선해양공학과 교수

Abstract : *Weight is a critical factor in the ship design process given that it has a substantial impact on the hydrodynamic performance of ships. Typically, ships are optimally designed for specific conditions with a fixed draft and displacement. However, in reality, weight and draft can vary within a certain range owing to operational activities, such as fuel consumption, ballast adjustments, and loading conditions . Therefore, we investigated how resistance changes under three different loading conditions, namely overload, design-load, and lightship, for small craft, using both model experiments and numerical simulations. Additionally, we examined the sensitivity of weight changes to resistance to enhance the performance of ships, ultimately reducing power requirements in support of the International Maritime Organization's (IMO) goal of reducing CO2 emissions by 50% by 2050. We found that weight changes have a more significant impact at low Froude Numbers. Operating under overload conditions, which correspond to a 5% increase in draft and an 11.1% increase in displacement, can lead to a relatively substantial increase in total resistance, up to 15.97% and 14.31% in towing tests and CFD simulations, respectively.*

Key Words : *Small craft, Towing test, Computational fluid dynamics (CFD), Resistance, Loading conditions*

요 약 : 선박의 설계과정에 있어, 선박의 중량은 유체역학적 성능에 큰 영향을 미치는 가장 중요한 요소 중 하나이다. 선박은 일반적으로 최적의 흘수와 배수량을 갖는 하나의 조건으로 설계되지만, 실제로는 연료의 소비, 선박 평형수의 충전과 적재 조건과 같은 운항 활동으로 인해 선박의 중량 및 흘수가 일정 범위 내에서 바뀐다. 본 연구에서는 소형선박을 대상으로 3가지 하중조건에 따른 선박의 저항성능 변화를 모형실험과 수치해석을 통해 연구하였다. 마지막으로 2050년까지 CO2 배출 가스를 50% 감축한다는 국제해사기구(IMO) 목표를 따라 선박의 저항 성능을 개선하여 동력 요구 사항을 줄이기 위해 선박의 중량 변화에 따른 저항성능의 민감도를 연구하였다. 연구 결과, 선박의 중량변화에 따른 효과는 낮은 프루드 수에서 크게 나타나는 것으로 확인되며, 저항성능에 대한 연구 결과, 설계 흘수의 적재조건을 기준으로 배수량이 11.1% 증가하고, 흘수가 5% 증가한 Over load의 적재조건에서 운항 시 선체의 총 저항이 모형시험과 CFD 시뮬레이션에서 각각 15.97%, 14.31%까지 증가하는 것을 볼 수 있다.

핵심용어 : 소형활주선박, 모형시험, CFD, 저항성능, 하중조건

* First Author : lognhorn15@gmail.com
† Corresponding Author : kcseo@mmu.ac.kr, 061-240-7303

1. Introduction

Ships are designed to complete and answer the requirements of the ship's owner, which can be concluded into one single operation scheme. This kind of philosophy causes a ship to be designed into one optimum condition to answer the purpose of the ship's presence. During the design process, weight and displacement are the most important factors to consider. A ship's main particulars are mainly chosen to be able to carry the weight or load within its limited working environment. This logic brings optimum ship characteristics such as length, breadth, height, and draught. Unlike other ship characteristics, draught is one of the parameters that is constantly changing due to many factors, such as fluid density, loading conditions, fuel consumption, stability problems, trim optimization, etc. Loading conditions are one of the factors that are unavoidable due to their natural changes during the operation. These changes mainly affect the ship's draught which is sensitively changing the ship's displacement, resulting in significant changes to the ship's hydrodynamic performance, such as resistance.

Many studies have been done to give a deeper understanding of this issue. A full-scale bulk carrier resistance assessment under different draughts is performed both using numerical and experimental studies (Farkas et al., 2018). Three different draughts are evaluated within various trim conditions on a container ship, aiming for an optimum condition in the actual navigation to reduce the ship's resistance by the CFD method which is later experimentally verified (Gao et al., 2019). A prediction of container ship resistance under different draught is also studied with Radial Basis Function Neural Network (RBFNN) and other machine learning models (Yang et al., 2021). In confined waters, a vessel's trim and draught are optimized to enhance the resistance characteristics of the KCS model using CFD (Campbell et al., 2022). Different displacement conditions of a planing catamaran are investigated by experimental and numerical methods to give a better understanding of the hydrodynamics of the vessel (Wang et al., 2022). Furthermore, the added resistance of a tanker in head waves for 4 different draughts is also studied experimentally and numerically. (Park et al., 2016).

Most of the recent studies are focused on the relatively big size of ships or displacement vessels, which commonly happens due to the natural behavior of loading conditions changing during its operation. However, draught changes on small ships (<499 GT) are commonly designed for semi-planing to the planing regime has a relatively big impact on its hydrodynamic performance.

For the relatively small size of ships, a simple empirical formula is provided to predict the planing hull resistance (Savitsky, 1964) where displacement plays a significant role by maintaining the equilibrium moment of weight and hydrodynamic lift. Several studies of resistance performance analysis to support the design modernization of small-size vessels, especially fishing boats are also widely explored (Kim and Lee, 1984) (Lee, 1984) (Lee et al., 2006) (Kang et al., 2007) (Yu and Lee, 2007). Also, small crafts are numerically studied under low-speed (Jee et al., 2009) and high-speed (Yu et al., 2011) to see the resistance performance.

Since it dominates up to 46% of the whole population of ships in the world (Equasis, 2020), this study aims to give a deeper understanding of the relationship between the loading conditions to the small craft's resistance. In conclusion, an improvement could be made to have a lower power requirement to reduce CO_2 gas emissions by up to 50% in alignment with the International Maritime Organization (IMO) goals for 2050 (IMO, 2018).

2. Methodology

In this study, three different speeds are analyzed under three different loading conditions. The study is performed both experimentally and numerically. The experimental analysis is performed in a high-speed towing tank facility under calm water conditions, while the numerical analysis is performed by a commercial Computational Fluid Dynamics (CFD) software of Simcenter Star-CCM+.

2.1 Target Vessel

A V-type planing hull form of a small craft with a 20-degree deadrise angle is used in this study. With the limitation of the towing tank facility, a final length of 1.972 m corresponding to a 1:9 scale is chosen. For the design load conditions, the ship's model has a 31.325 kg displacement with 0.116 m draught. At the stern section, an improvement to increase the inflow to the propeller region is made by using a flat-roof tunnel stern, while a center keel is used in the centerline for stability. A linesplan of the small craft used as the target vessel is shown in Fig 1.

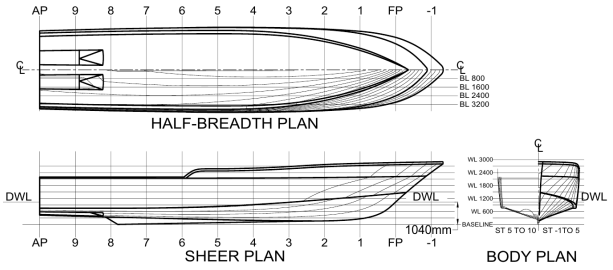

Fig. 1. Target vessel's linesplan.

Table 1. Full scale and model scale of the small craft main particulars at design load

Item	Full Scale		Model	
	Value	Unit	Value	Unit
Length overall	17.749	m	1.972	m
Breadth	3.703	m	0.412	m
Design draught	1.040	m	0.116	m
Design displacement	22.836	ton	31.325	kg
Deadrise	20	deg.	20	deg.
Waterplane coefficient	0.749	-	0.749	-

2.2 Study Cases

The changes in loading conditions are made by changing the draught of the targeted vessel while maintaining other parameters to be fixed. Three loading conditions of overload, design load, and lightship are made by changing the vessel's draught (T) ranging from 0.96T to 1.05T, which is shown in Fig. 2.

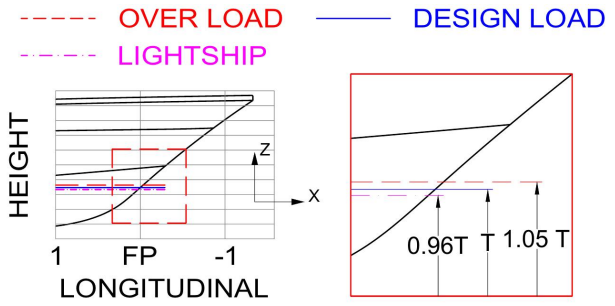

Fig. 2. Draught changes under different loading conditions.

Table 2. Small craft under different loading conditions

Loading conditions	Disp. (Δ)	Draught (T)	C_{WP}	F_N
Over load	111%	1.05T	0.755	0.56,
Design load	100%	T	0.749	0.63,
Lightship	90.6%	0.96T	0.742	0.91

The resistance evaluation is made within the range of Froude Number of 0.56 ~ 0.91 to see the effect of each loading condition within the semi-planing to planing speed range. Therefore, a total of 3 different loading conditions were performed at 3 different speeds resulting in a total of 9 cases which are summarized in Table 2. Where draught is defined as T which is mentioned in Table 1, and C_{WP} is the waterplane area coefficient. The waterplane area coefficients are within the range of 0.742 ~ 0.755, which is varied due to the changes in the bow section. With a relatively uniform stern section, there are no significant changes in waterplane form in the stern area. By increasing the vessel's draught up to 5%, an overload condition with an 11% increase in displacement is achieved, while reducing the draught by 4% or corresponding to the lightship condition, a reduction of 9.4% displacement is achieved.

3. Model Test Experiment

A 1.972 m long small craft model is made with glass-fiber material, with foam composite for the construction. Five transverse frames and a deck edge ring frame are equipped to support the transverse and torsional stiffness. Thin mylar strips which are shown in Fig. 3, are added to the chine region to maintain the edge sharpness, which can separate the transverse flow. Additionally, solid wood mounting pads are installed as the measuring instrumentation seating, and two ballast weight pads are to support the changes in the ship's loading conditions. The weight is equally distributed along the ship model to maintain the center of gravity. The model setup is presented in Fig. 4 below.

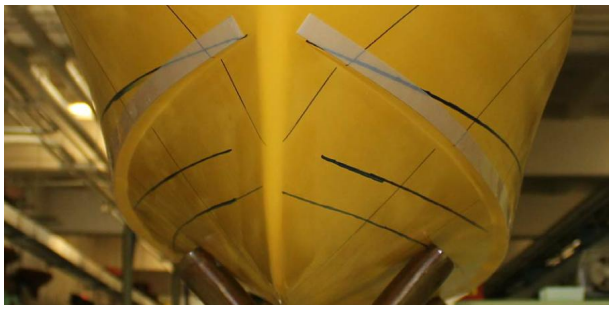

Fig. 3. Mylar strips at the chine region.

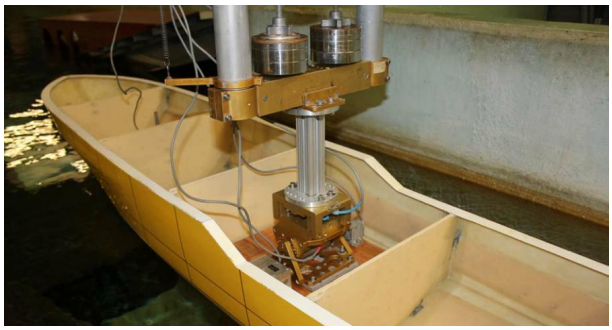

Fig. 4. Towing test experiment model setup.

3.1 Towing Tank Conditions and Measurement

The towing test experiment is conducted in the high-speed towing tank 3 at the Davidson Laboratory, which is 95 m long by 5 m wide, and 2 m deep. The towing test facility is equipped with an electric motor with steel cable driven located above the center of the water tank. The towing carriage rides the monorail while the model is free to heave and pitch but fixed in other degrees of motion. The towing test experiments are performed for all cases with the towing test conditions as summarized in Table 3 below, as aligned with the ITTC guidelines and procedures to ensure the reliability of the test results (ITTC, 2014a) (ITTC, 2021).

The instrumentations for resistance measurement are calibrated with the ITTC procedure (ITTC, 2017) before being used in the experiments. LVDT-based linear drag balance instruments are used for resistance evaluation, while the trim and speed are measured by Schaevitz-type linear servo inclinometer and linear quadrature encoder or PC-based clock, respectively. An absolute reading difference of 0.09 N for drag and 0.06 degrees for trim is recorded, which can be concluded as tolerable, and the device is well-calibrated and the towing test experiments are ready to be performed.

Table 3. Towing tank facility conditions

Parameters	Value
Dimensions (length x breadth x depth)	95 x 5 x 2 m
Model scale	1:9
Fluid type	Fresh water
Fluid temperature	21.111 °C
Fluid density	997.774 kg/m^3
Kinematic viscosity	9.75 x 10^{-7} m^2/s

3.2 Model Test Results

The towing test experiments are performed for all considered cases. The total resistance is measured and summarized in Table 4. Along with the displacement and draught reduction, the resistance is reduced. This is easily known by the reduction length of waterline as shown in Fig. 2, which also reduced the wetted surface area.

In Froude Number 0.56, changing load conditions from design load to overload condition gives a significant increase in resistance of up to 15.97%, while getting lower by up to 10.39% at Froude Number 0.91. Also, the resistance is greatly reduced by up to 11.07% by operating in lightship condition compared to the design load at the Froude Number 0.56 and reduced up to 9.27% at the Froude Number 0.91 for equivalent loading condition changes.

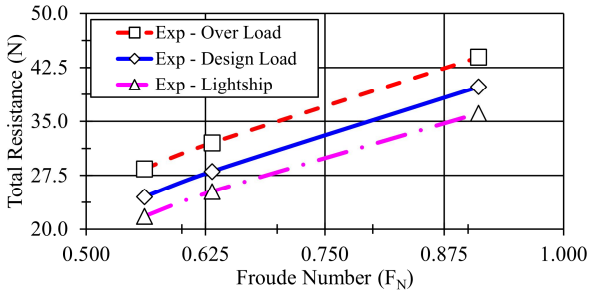

Fig. 5. Total resistance measured by towing test experiments.

Table 4. Total resistance changes under different loading conditions measured by towing test experiments

Loading Conditions	Froude Number	Total Resistance	
(-)	(-)	(N)	(%)
Over Load	0.56	28.424	115.97
Design Load		24.510	100.00
Lightship		21.796	88.93
Over Load	0.63	32.027	114.10
Design Load		28.068	100.00
Lightship		25.266	90.02
Over Load	0.91	43.948	110.39
Design Load		39.811	100.00
Lightship		36.119	90.73

The trend of resistance changes under different loading conditions is presented in Fig. 5. Loading conditions play an important role in every speed regime. Gives a significant increment of 10.39% - 15.97% by operating in an overload condition, and a reduction of 9.27% - 11.07% by operating in a lightship condition.

4. Numerical Analysis

Computational Fluid Dynamics (CFD) is a fluid mechanic-based software that can perform fluid flow problems with numerical analysis. In this study, commercial CFD software Simcenter Star-CCM+ is used to perform the analysis. CFD analysis is commonly used since it could capture the flow analysis better, and

the sensitivity could be used to accommodate small changes in the ship design process with relatively less computational time compared to the towing test method.

4.1 Methodology

In recent studies, several methods are usually used for planing ship resistance evaluation, which targets the accuracy of the simulations. Reynolds-averaged Navier-Stokes (RANS) equations are commonly used as the governing equations for the viscous fluids within a time function in a finite volume, which can be seen in the equations below.

$$\frac{dV}{dt}+\oint_{S(t)} dS \cdot (u-v)=0 \tag{5}$$

$$\frac{d}{dt}\int_{V(t)} u\,dV=\oint_{S(t)} dS \cdot \overline{T} \tag{6}$$

$$\overline{T}=-(u-v)u-P\bar{I}+v\left[\nabla u+(\nabla u)^T\right] \tag{7}$$

Where dV is the volume element, t is the time, $S(t)$ is the surface area vector, dS is a surface area element, u is the velocity vector, and v is the surface element velocity resulting from the motion of volume control. $\overline{T}$ is the stress tensor, P is the pressure, and $\bar{I}$ is the identity tensor, ∇u is the gradient of u and superscript $(.)^T$ is the matrix transpose operator (Rosenfeld and Kwak, 1991).

To simulate the turbulence flow characteristics, a modified turbulence model of SST-k-ω is used (Menter, 1994). This model could provide better accuracy at the boundary layer. The equations are presented as follows:

$$\frac{D\rho k}{Dt}=\tau_{ij}\frac{\delta u_i}{\delta x_j}-\beta^*\rho\omega k+\frac{\delta}{\delta x_j}\left[(\mu+\sigma_\omega\mu_t)\frac{\delta_\omega}{\delta x_j}\right] \tag{8}$$

$$\frac{D\rho\omega}{Dt}=\frac{\Upsilon}{v_t}\tau_{ij}\frac{\delta u_i}{\delta x_j}-\beta\rho\omega^2+\frac{\delta}{\delta x_j}\left[(\mu+\sigma_\omega\mu_t)\frac{\delta\omega}{\delta x_j}\right] +2\rho(1-F_1)\sigma_{\omega 2}\frac{1}{\omega}\frac{\delta k}{\delta x_j}\frac{\delta\omega}{\delta x_j} \tag{9}$$

This turbulence model is derived by transforming the standard model of high-Reynolds-number k-ε to a k-ω turbulence model by applying multiplier blending factor of F_1 or $(1\text{-}F_1)$. Several constants which used in this turbulence models are $\sigma_{k1}=0.5$, $\sigma_{w1}=0.5$, $\beta_1=0.075$, $\beta^*=0.09$, $\kappa=0.41$, $\sigma_{k2}=1.0$, $\sigma_{w2}=0.856$, $\beta_2=0.0828$, $\gamma_1=\beta_1/\beta^*-\sigma_{w1}\kappa^2/\sqrt{\beta^*}$, $\gamma_2=\beta_2/\beta^*-\sigma_{w2}\kappa^2/\sqrt{\beta^*}$.

To get the real condition of ship operation, the ship experiences resistance from multiphase fluids, namely water, and air. The free-surface area is defined as the region where the air and fluids are met, which in this case is the small craft's draught. The complexity of this free surface is captured with High-Resolution Interface Capturing (HRIC), while the fluids are modeled using the multiphase model included in the CFD package. The volume of Fluid (VOF) is used to divide the heavy and light fluid of water and air by a volume fraction, between the range of 0 to 1 $(0<F<1)$.

The loading conditions are simulated by changing several settings in the physics setup. First, the flat volume of the fluid wave (flat VOF wave) is used to model calm water conditions. The draught changes are applied by changing the point of the water level. Second, the displacement changes are set in the Dynamic Fluid Body Interaction (DFBI) settings, where the hull is set into a 3D continuum body, and the mass could be adjusted under this setting, along with the moment of inertia of the hull. The physics setup and configuration used in this study are listed in Table 5.

Table 5. Physics setup

Methodology	Model
Equation	Reynolds-averaged Navier Stokes
Turbulent model	SST-$k-\omega$
Multiphase	Volume of Fluid
Free surface	HRIC scheme
Body motion	DFBI (heave and pitch) free motion
Time step	Implicit unsteady

For validation and verification, a recent study of a planing ship (Begovic and Bertorello, 2012) is used. This study provides the hull geometry along with the towing test result. In this process, the Warped-2 hull form is chosen among the hull forms. The Warped-2 hull form is a single chine v-type hull form which is chosen since it has relatively similar characteristics to the target vessel. With a length of 1.900 m, breadth of 0.424 m, and draught of 0.110 m, a displacement of 32.630 kg is achieved.

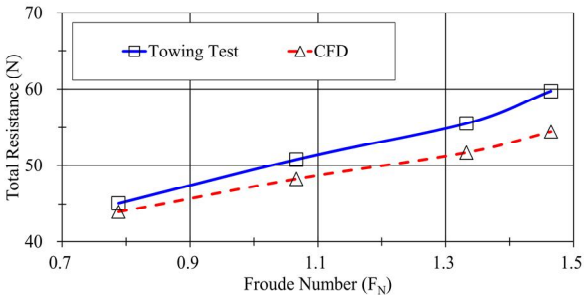

Fig. 6. Total resistance comparison of Warped - Hull 2.

The verification process is performed at 4 different speeds and the results are shown in Fig. 6, where the total resistance and is chosen as the parameter for the comparison, respectively. An average difference of 5.80% of total resistance is occurred. Considering the reasonable results, the same physic setup will be applied to the small craft as the target vessel.

4.2 Computational Domain and Boundaries

To reduce the computational time, the towing test is designed as small as possible but still large enough to capture the flow, and to avoid the reverse flow into the domain. Therefore, International Towing Tank Conference (ITTC) procedures and guidelines (ITTC, 2014b) are taken into consideration. The computational domain and boundaries is presented in Fig. 7 below.

The numerical analysis is performed for a half section of the vessel port-side since it will give similar results for the starboard side. This method could reduce the computational time by reducing the number of cells, which can be done by applying symmetry plane boundaries in the ship's geometry centerline. Followed by velocity inlet for the inlet, side, bottom, and top regions, and pressure outlet for the outlet regions. The hull geometry is set to wall regions, with overset boundaries made around the hull.

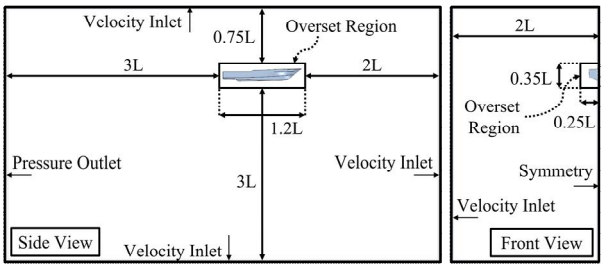

Fig. 7. Computational domain and boundaries.

4.3 Mesh Configurations

The mesh configuration is one of the factors that need to be considered in the numerical simulations. In this study, overset mesh is used to reduce the number of cells in the simulations. Overset region is an adaptive meshing strategy that consists of donor cells and adaptor cells, which create a continuous layer by transforming information from cell to cell. Prism layer mesh is used around the boundary layer of hull regions with all y+ treatment methods, with a value of greater than 40 ($y^+ > 40$). Richardson's extrapolation (Richardson, 1927) is used to consider the optimum mesh size. Three sizes of meshes are considered, and finally resulting a mesh consisting of 2.57 million cells is created along with the volume control for the free surface and wake region refinement.

4.4 Numerical Simulation Results

The CFD analyses are performed for all considered cases, and the results are summarized in Table 6 below. The results are reasonably satisfactory since it has the same trend as the towing test results. A potential total resistance reduction of up to 11.28% was achieved at Froude Number 0.56, and 8.49% at Froude Number 0.91, by changing load conditions from design load to lightship.

Table 6. Total resistance changes under different loading conditions measured by CFD simulations

Loading Conditions	Froude Number	Total Resistance	
(-)	(-)	(N)	(%)
Over Load	0.56	27.915	114.31
Design Load		24.421	100.00
Lightship		21.668	88.72
Over Load	0.63	31.262	113.28
Design Load		27.597	100.00
Lightship		24.619	89.21
Over Load	0.91	43.107	110.94
Design Load		38.857	100.00
Lightship		35.557	91.51

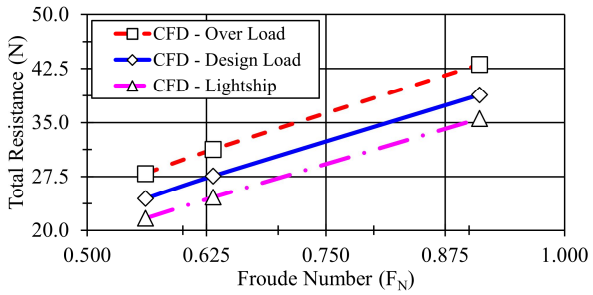

Fig. 8. Total resistance measured by CFD simulations.

The trend of resistance changes under different loading conditions is presented in Fig. 8. The trend is similar to the towing test experiments which are previously done. Gives a significant increment of 10.94% - 14.31% by operating in an overload condition.

5. Results and Discussion

Both analyses are performed based on the guidelines and present studies for both experimental and numerical analysis. The results show a similar trend for all considered cases. Within all test conditions, CFD analyses always underperformed compared to the towing test experiment. As summarized in Table 7, a maximum difference of -2.625% while as close as a -0.361% difference was achieved between the CFD analysis and towing test experiment. Therefore, the CFD results are reliable and could be used to perform further analysis during the design process.

In a higher Froude Number of 0.91, the difference gap tends to get wider compared to the lower Froude Number of 0.56. This phenomenon could be described as a Numerical Ventilation (NV) problem due to mesh sensitivity and the time-step of the simulation. This leads to a reduction in friction resistance which results in lower total resistance.

The resistance evaluation is considered reasonably satisfactory and well simulates the towing test experiment as shown in Fig. 9. The resistance measured by both methods gives a similar trend. While the towing test method could capture the resistance increment of 15.97% at the low Froude Number of 0.56, the CFD results show similar results of 14.31%. Not only giving the same trend of increment, total resistance is reduced by up to 11.07% by the towing test method, and the CFD simulations of up to 11.28% for the same condition, proving that CFD simulations are considered reliable to perform further analysis. Giving a maximum resistance trend differences of 1.66% and as close as 0.20%.

The resistance changes are more sensitive in lower Froude Number and could be theoretically proven. The fact that most of the resistance consists of frictional resistance which is mainly affected by the wetted surface area. Operating in the low-speed regime of Froude Number 0.56 tends to give a smaller hydrodynamic lift. With the absence of a hydrodynamic lift, the displacement of the vessel is dominant, and the bow is not sufficiently lifted, resulting in a longer length of waterline and a bigger wetted surface area. Therefore, in conclusion, by reducing the displacement by changing loading conditions in this speed regime, the resistance which mainly depends on the displacement could be highly reduced. While in the higher speed regime, a hydrodynamic lift is significantly produced, resulting in a shorter waterline and smaller wetted surface area. The displacement is greatly supported by the hydrodynamic lift, therefore, reducing the displacement will not affect as much as in low Froude Number.

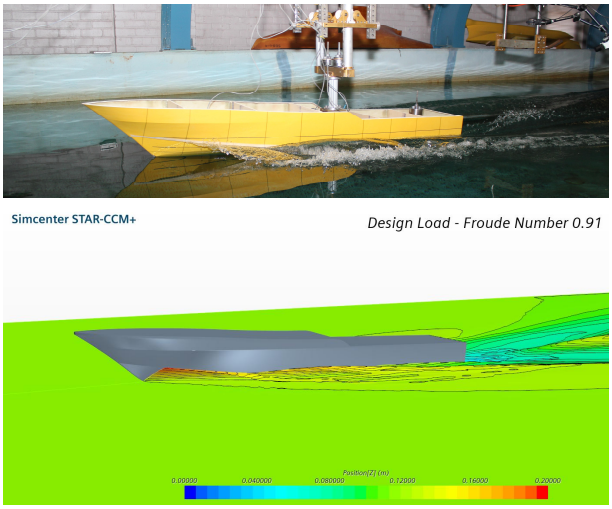

Fig. 9. Towing test (top), and CFD simulations (bottom) of small planing ship at design load in Froude Number 0.91.

6. Conclusion

This study concludes the effect of changing loading conditions on small craft resistance by towing test and CFD simulations. The total resistance of CFD simulations is underperformed compared to the towing tests, ranging from 0.36% – 2.63% less than towing test method. While comparing the trend of resistance changes, a maximum of 1.66% while as close as 0.20% is shown at the low Froude Number of 0.56. These results are considered satisfactory and the CFD simulations are reliable for further study.

Table 7. Total resistance changes under different loading conditions by towing test experiment and computational fluid dynamics (CFD)

Loading Conditions	F_N	Towing Test Experiment			Computational Fluid Dynamics (CFD)			Trend Difference
		Total Resistance (R_T)		Difference (A)	Total Resistance (R_T)		Difference (B)	(A) - (B)
(-)	(-)	(N)	(%)	(%)	(N)	(%)	(%)	(%)
Over Load	0.56	28.424	115.97	15.971	27.915	114.31	14.307	1.663
Design Load		24.510	100.00	-	24.421	100.00	-	-
Lightship		21.796	88.93	-11.071	21.668	88.72	-11.275	0.205
Over Load	0.63	32.027	114.10	14.105	31.262	113.28	13.281	0.823
Design Load		28.068	100.00	-	27.597	100.00	-	-
Lightship		25.266	90.02	-9.984	24.619	89.21	-10.788	0.804
Over Load	0.91	43.948	110.39	10.391	43.107	110.94	10.938	-0.547
Design Load		39.811	100.00	-	38.857	100.00	-	-
Lightship		36.119	90.73	-9.274	35.557	91.51	-8.493	-0.781

The weight sensitivity is more dominant in the lower Froude Number of 0.56 compared to the higher Froude Number of 0.91. Operating in an overload condition, or corresponding to an increase of the draught by 5%, could result in 11.1% more displacement, and could add as high as 15.97% to the total resistance. The same phenomenon also happened by operating in a lightship. Reducing the draught by 4.3%, resulting in a 9.4% reduction of displacement, could reduce the resistance to up to 11.07%.

These happened due to the fact that in the low Froude Number, displacement plays a big role in the hydrodynamic performance since the hydrodynamic lift is lowly produced. Therefore, a greater wetted surface area and longer length of waterline is achieved. While in the higher Froude Number, the displacement is mainly supported by the hydrodynamic lift. Therefore, reducing the displacement in this speed regime gives a relatively smaller change to the hydrodynamic performance, compared to the lower Froude Number.

A wider speed range and hull-form type are to be considered in further study. Due to limitations of time, only several loading conditions under specific hull-types and speeds are considered in this study. However, in fact, the potential of resistance changes under different loading conditions may vary between each hull form. In addition, the potential of loading conditions under different longitudinal centers of gravity (LCG) are also to be considered in the future due to the complexity of the equilibrium moment of weight acting on the center of gravity (CG) and hydrodynamic lift acting on the center of buoyancy (CB).

Acknowledgment

This research was supported by a grant (20015029) of Regional Customized Disaster-Safety R&D Program, funded by Ministry of Interior and Safety (MOIS, Korea).

References

[1] Begovic, E. and C. Bertorello(2012), Resistance assessment of warped hullform. Ocean Engineering, 56, pp. 28-42.

[2] Campbell, R., M. Terziev, T. Tezdogan, and A. Incecik(2022), Computational fluid dynamics predictions of draught and trim variations on ship resistance in confined waters. Journal of Applied Ocean Research, 126, 103301.

[3] Equasis(2020), The 2020 world merchant fleet statistics from Equasis. Saint-Malo: Equasis.

[4] Farkas, A., N. Degiuli, and I. Martic(2018), Assessment of hydrodynamic characteristics of a full-scale ship at different draughts. Journal of Ocean Engineering, 156, pp. 135-152.

[5] Gao, X., K. Sun, S. Shi, B. Wu, and Z. Zuo(2019), Research on influence of trim on a container ship's resistance performance. Journal of Physics: Conference Series, 1300, 012015.

[6] IMO(2018), Guidelines on the method of calculation of the attained energy efficiency design index (EEDI) for new ships. Marine Protection Environment Committee, MEPC.212(63).

[7] ITTC(2014a), ITTC - Recommended Procedures and Guidelines - General Guideline for Uncertainty Analysis in Resistance Tests (7.5-02-02-02). International Towing Tank Conference.

[8] ITTC(2014b), ITTC - Recommended Procedures and Guidelines - Practical Guidelines for Ship CFD Applications (7.5-03-02-03). International Towing Tank Conference.

[9] ITTC(2017), ITTC - Recommended Procedures and Guidelines - Uncertainty Analysis: Instrument Calibration (7.5-01-03-01). International Towing Tank Conference.

[10] ITTC(2021), ITTC - Recommended Procedures and Guidelines - Example for Uncertainty Analysis of Resistance Tests in Towing Tanks (7.5-02-02-02.1). International Towing Tank Conference.

[11] Jee, H., Y. Lee, D. Kang, Y. Ha, Y. Choi, and J. Yu(2009), Resistance performance of Korean small coastal fishing boat in low-speed range, Journal of the Society of Naval Architects of Korea, 46(1), pp. 10-23.

[12] Kang, D., J. Yu, and Y. Lee(2007), A study on the hull form design with minimum resistance for domestic coastal fishing boats. Journal of the Soecity of Naval Architects of Korea, 44(4), pp. 349-359.

[13] Kim, H. and Y. Lee(1984), Research on modernization of small fishing boats. KIMM.

[14] Lee, Y.(1984), A study on the EHP estimation and design procedure of small fishing boat's hull form. Bulletin of the Society of Naval Architects of Korea, 21(3), pp. 1-10.

[15] Lee, Y., J. Yu, K. Kim, and D. Kang(2006), A study on the effecitve horsepower estimation for domestic coastal fishing vessels. Journal of the Society of Naval Architects of Korea, 43(3), pp. 313-321.

[16] Menter, F. R.(1994), Two-equation eddy-viscosity turbulence models for engineering applications. AIAA Journal, 32(8), pp. 1598-1605.

[17] Park, D. -M., Y. Kim, M. -G. Seo, and J. Lee(2016), Study on added resistance of a tanker in head waves at different drafts. Journal of Ocean Engineering, 111, pp. 569-581.

[18] Richardson, L. F.(1927), The deferred approach to the limit. Transactions of the Royal Society of London, 226, pp. 299-361.

[19] Rosenfeld, M. and D. Kwak(1991), Time-dependent solutions of viscous incompressible flows in moving co-ordinates. International Journal for Numerical Methods in Fluids, Volume 13, pp. 1311-1328.

[20] Wang, H., R. Zhu, L. Zha, and M. Gu(2022), Experimental and numerical investigation on the resistance characteristics of a high-speed planing catamaran in calm water. Journal of Ocean Engineering, 258, 111837.

[21] Yang, Y., H. Tu, L. Song, L. Chen, D. Xie, and J. Sun(2021), Research on accurate prediction of the container ship resistance by RBFNN and other machine learning algorithms. Journal of Marine Science and Engineering, 9(4), 376.

[22] Yu, J. and Y. Lee(2007), A study on the bow wave characteristics for the resistance-minimized hull form of small fishing boat. Journal of the Society of Naval Architects of Korea, 45(2), pp. 124-131.

[23] Yu, J., Y. Lee, A. Park, Y. Ha, C. Park, and Y. Choi(2011), A study on the resistance performance of Korean high-speed small coastal fishing boat. Journal of the Society of Naval Architects of Korea, 48(2), pp. 158-164.

Received : 2023. 09. 20.
Revised : 2023. 10. 24.
Accepted : 2023. 10. 27.